Int J Clin Exp Pathol 2013;6(8):1467-1480
www.ijcep.com /ISSN:1936-2625/IJCEP1304038

*Original Article*

# Histopathological and functional effects of antimony on the renal cortex of growing albino rat

Ahmed H Rashedy[1], Adnan A Solimany[2], Ayman K Ismail[3,4], Mohamed H Wahdan[5], Khalid A Saban[6]

*[1]Department of Pathology, College of Medicine, Taif University, KSA; [2]Department of Pediatric, College of Medicine, Taif University, KSA; [3]Departments of Forensic Medicine and Toxicology, College of Medicine, Taif University, KSA; [4]Departments of Forensic Medicine and Toxicology, Suez Canal University, Egypt; [5]Department of Anatomy, College of Medicine, Taif University, KSA; [6]Department of Nuclear Medicine, College of Medicine, Taif University, KSA*

Received April 28, 2013; Accepted July 9, 2013; Epub July 15, 2013; Published August 1, 2013

**Abstract:** Contamination of the environment with antimony compounds may affect human health through the persistent exposure to small doses over a long period. Sixty growing male albino rats, weighing 43-57 grams, utilized in this study. The animals were divided into 3 groups; each of 20 rats: animals of group I served as control, animals of group II received 6 mg/kg body weight antimony trisulfide daily for 8 weeks with drinking water, and those of group III received the same dose by the same route for 12 weeks. The Malpighian renal corpuscles showed distortion, destruction and congestion of glomerular tuft, vacuoles in the glomeruli, peritubular haemorrhage, obliteration of Bowman's space, and thickening with irregularity of Bowman's membrane. The proximal convoluted tubules demonstrated patchy loss of their brush border, thickening of the basement membrane with loss of its basal infoldings, disarrangement of the mitochondria, pleomorphic vacuoles in the cytoplasm, apical destruction of the cells, apical migration of the nuclei, and absence of microvilli. On the other hand, peri-tubular hemorrhage, apical vacuolation, small atrophic nuclei, swelling of mitochondria, obliteration of the lumina, destruction of cells, and presence of tissue debris in the lumina, were observed in the distal convoluted tubules. The present work demonstrated the hazardous effect of antimony on the renal function as evidenced by the significant increase of the level of blood urea, serum creatinine, and serum sodium and potassium. In conclusion, this study proposed that continuous oral administration of antimony for 8 and 12 weeks has hazardous toxic effect on the structure and function of the kidney in growing albino rat. Based on the results of the present study, it is recommended to avoid the use of any drinking water contaminated with antimony compounds and forbidden its use in infants and children foods.

**Keywords:** Antimony, histopathology, blood chemistry, renal cortex, growing albino rat

## Introduction

The effect of antimony on the various regions of the genitor-urinary system of albino rats has been conventionally described by many authors [1-3] but the information available from the literature about its effect on the kidney is still lacking and controversial.

There has been a major resurgence of interest in antimony toxicity with numerous publications in both the scientific and lay press [4]. Comprehensive reviews have recently been published on the effects of antimony exposure on the human infants, children and adults [5], on antimony nephrotoxicity [6], on antimony hepatotoxicity, on antimony encephalopathy [7], on antimony chronic peripheral neuropathy [8], on antimony genotoxic effects [2], and on the postnatal growth produced by antimony [9].

Clearly, antimony is a major environmental toxin due to its presence in air, water, food and soil [10]. Antimony and its compounds may be used in the manufacture of paints, coatings, rubber, insecticides, colored printing inks and glass [11]. Human beings have always been exposed to antimony but its amount is substantially increased due to industrial production [12]. Other major antimony sources include metal smelters, mining, cement production and garbage burden [13]. Antimony toxicity occurs

either due to occupational exposure or during therapy [14]. Occupational exposure may cause gastrointestinal symptoms, antimony spots on the skin, respiratory irritation and pneumoconiosis [8]. In addition, antimony trioxide is possibly carcinogenic to humans [13]. Antimony has been mostly used for the treatment of leishmaniasis and schistosomiasis and its major toxic side effects are cardiotoxicity and pancreatitis [15].

High doses of antimony were toxic in rats as well as in humans and it acted mainly on the endothelial cells of the blood vessels of kidney, liver and central nervous system [1]. This caused an increase in capillary permeability to blood cells and proteins with vasogenic edema [16]. On the other hand, low doses of antimony did not increase capillary permeability to blood cells and proteins, but it could affect the normal function of endothelial cells by affecting the transport of some important metabolites [17]. Haemorrhage in the kidney, liver, suprarenal gland, gonads, cerebellum, spinal cord and cerebral hemispheres have been recorded [18]. Rats administered antimony had the highest concentration of antimony in the renal cortex at all age and dose groups [14]. This made the renal cortex one of the most vulnerable areas of antimony toxicity [8]. On the contrary, presence of any antimony toxicity on the renal cortex of albino rats was denied by others [19].

Although most of the available researches dealt with the biochemical effects of antimony on the different organs; however few of them described the gross morphological changes induced by antimony on these organs and since there is only little information about the effects of antimony on the structure and function of the kidney and its possible nephrotoxicity. Therefore, the aim of the current study is to elucidate the possible deleterious effects of continuous oral exposure to small dose of antimony that would not alter the growth and body weight of growing male albino rats on the structure and function of the renal cortex of these rats and to find out the possible carcinogenic effect of this heavy metal.

## Material and methods

This study was carried on 60 growing male albino rats of Sprague Dawley strain. Their weight ranged between 43 and 57 grams. They were housed individually in well-aerated metal cages under standard conditions and were fed on a balanced powdered laboratory chow and distilled water ad libitum.

In this study, antimony trisulfide crystals 100%, obtained from *El-Nasr Chemical Company*, Cairo, Egypt were used and dissolved in distilled water at concentration (6%) [20]. It was in the form of white crystalline powder, dissolved in distilled water, and given with drinking water to the experimental animals (groups II & III).

Animals divided into three groups each of 20 rats: Group I (Control group) received no medication and lived in the same environment. It was divided into two equal subgroups: Subgroup Ia and subgroup Ib drank distilled water free from antimony for 8 and 12 weeks respectively. While Group II received 6 mg/kg body weight antimony trisulfide daily for 8 weeks [7]. Group III received 6 mg/kg body weight antimony trisulfide daily for 12 weeks [21].

*Histological study*

At the end of the experimental periods, the animals were sacrificed by cervical decapitation. The anterior abdominal wall was opened by midline incision. The kidneys were carefully dissected and their cortices were relieved. Each renal cortex was divided into two specimens. The first specimen was fixed in formol-saline 10% for light microscopy, processed to get paraffin sections, and stained with Periodic Acid Schiff and Toluidine blue stains [22, 23].

The second specimen was fixed in 3% gluteraldehyde with 0.1 phosphate buffer (at pH 7.2), for 2 hours at room temperature for electron microscope processing. Specimens were then post-fixed in 1% osmium tetroxide in phosphate buffer (pH 7.2) for 2 hours at 4°C. After fixation, dehydration with ascending grades of ethanol and clearing using propylene oxide were performed. Specimens were embedded in Epon.

Semithin sections were cut at 1 μm thickness by ultracut Reichert JUNG ultra-microtome with the aid of glass knives, stained with toluidine blue and examined by Zeiss Axiophot light microscope to detect the areas of interest. Ultrathin sections (50 nm) were prepared using the same ultra-microtome and new glass knives

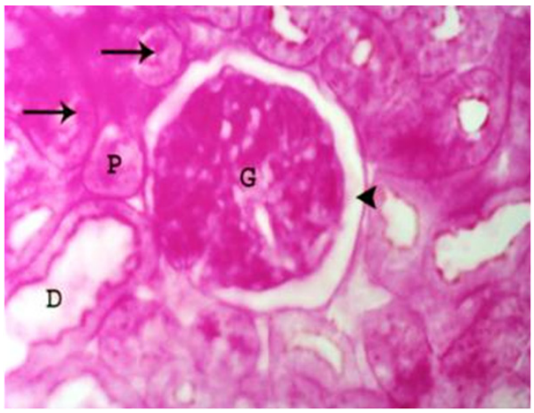


**Figure 1.** A photomicrograph of a section of a renal cortex of a control albino rat, showing normal structure of the glomerulus (G), proximal (P) and distal (D) convoluted tubules with PAS positive brush border (arrows). Normal Bowman's space (arrow head) can be seen (PAS reaction, X 400).

and stained with uranyl acetate for 20 minutes and lead citrate for 10 minutes [24]. These ultrathin sections were examined by Philips 400 T *transmission* electron microscope and photographed under different magnifications

*Laboratory study*

After scarification of the animals, blood was collected from the descending aorta and centrifuged for separation of its serum. Serum was transferred into clean quite fit plastic tubes and kept frozen at -20°C until analyzed for; serum blood urea, serum creatinine, serum potassium, serum sodium.

*Statistical analysis:* Data were expressed as mean values±SD of 10 replicate determinations. Statistical analysis was performed using one-way analysis of variance (ANOVA) to assess significant differences among treatment groups. The criterion for statistical significance was set at $p<0.05$ or $p<0.01$. All statistical analyses were performed using SPSS statistical version 8 software package (SPSS, Inc., USA).

## Results

*Histological results*

*Groups I:* No structural difference could be detected between rats of control kidneys. PAS reaction revealed the normal glomeruli, preserved Bowman's space and proximal and distal convoluted tubules with normal PAS positive brush border and narrow lumen (**Figure 1**).

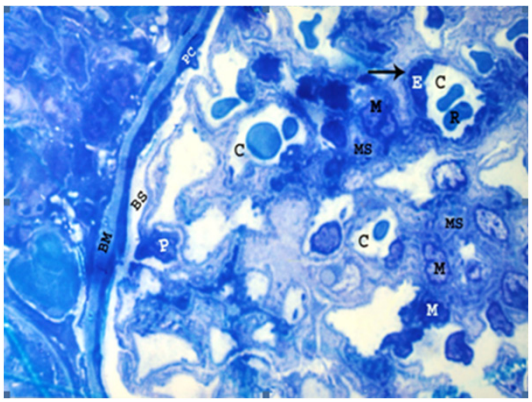


**Figure 2.** A photomicrograph of a semithin section of a renal cortex of a control albino rat, showing glomerular capillaries (C), some of which containing red blood cells (R). Capillary endothelial cells (E) are occasionally seen bulging into the capillary lumen and resting on thin basement membrane (arrow). Mesangium which consists of mesangial cells (M) and extracellular substance called mesangial substance (MS), can be observed. The surface of the glomerular capillaries exposed to Bowman's space (BS) is invested by visceral layer of Bowman's capsule i.e. podocytes (P). The parietal cells (PC) of Bowman's capsule are also seen resting on thin Bowman's membrane (BM) (Toluidine blue, X 1000).

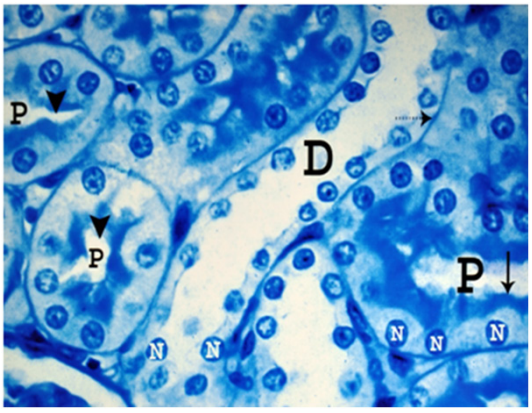


**Figure 3.** A photomicrograph of a semithin section of a renal cortex of a control albino rat, showing the cells of proximal convoluted tubules (P) with their rounded basal nuclei (N), indistinct cell boundaries and well defined luminal brush border (arrow). Note the narrow lumen (arrow head) of the tubules. The distal convoluted tubule (D) revealed wider lumen and are lined by a single layer of cuboidal cells laying on clear basement membrane (dotted arrow) with indistinct cell boundaries. Note rounded nuclei (N) and indistinct luminal brush border (Toluidine blue; X 1000).

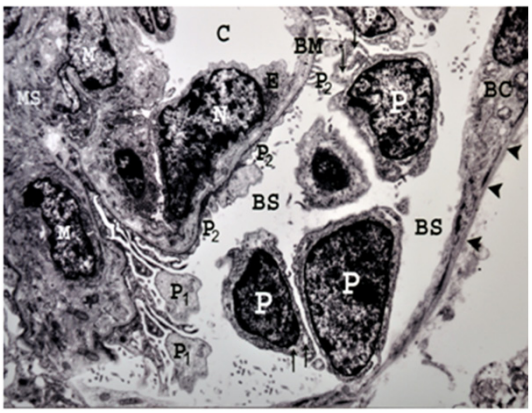


**Figure 4.** An electron micrograph of a renal cortex of a control albino rat showing glomerular capillary (C) which is lined by endothelial cells having a thin layer of cytoplasm (E) and a large nucleus (N) bulging into the capillary lumen. Note the mesangial cells (M) and mesangial substance (MS) support the capillary wall. The large nuclei of several podocytes (P), are surrounded by cytoplasm containing rough endoplasmic reticulum (arrows) and their primary processes ($P_1$) giving rise to numerous secondary foot processes ($P_2$) which rest on the glomerular capillary basement membrane (BM). Part of parietal layer of Bowman's capsule (BC), resting on regular Bowman's membrane (arrow heads) and Bowman's space (BS) are also seen (Uranyl acetate and lead citrate X 5000).


**Figure 5.** An electron micrograph of a renal cortex of a control albino rat, showing a proximal convoluted tubule with thin regular basement membrane (BM) which exhibits basal infoldings (arrows) closely related to columns of parallel elongated mitochondria (M). The basement membrane (BM) is separating the cells of the tubule from the delicate capillary (C). The cytoplasm immediately beneath the prominent microvilli (MV) contains many pinocytic vesicles (PV) and lysosomes (L). Note the large nucleus (N) with peripheral chromatin condensations (Uranyl acetate and lead citrate X 5000).

Light microscopic examination of semithin sections of the renal cortices of the control and sham control rats showed normal Malpighian renal corpuscles, proximal and distal convoluted tubules (**Figures 2**-**4**). The Malpighian corpuscles were formed of a central tuft of glomerular capillary loops surrounded by a Bowman's capsule. Each glomerular capillary loop consisted of thin basement membrane lined by flat endothelium surrounding a capillary lumen (**Figure 2**). Each Bowman's capsule was formed of flat visceral epithelial cells (podocytes) and Bowman's membrane which appeared thin, regular and lined by a single layer of flat parietal epithelial cells (**Figure 2**). The Bowman's space between the parietal and visceral layers was preserved and clears of any cell debris (**Figure 2**). Mesangium forming of mesangial cells and mesangial substance surrounded the capillary loops (**Figure 2**). The proximal convoluted tubules were lined by a single layer of pyramidal cells resting on a clear basement membrane with indistinct cell boundaries and narrow lumen. Each cell contained a large rounded basal nucleus and well defined luminal brush border (**Figure 3**). The distal convoluted tubules revealed wider lumina and were lined by a single layer of cuboidal cells laying on clear basement membrane with indistinct cell boundaries. Each cell contained a rounded central nucleus with indistinct luminal brush border (**Figure 3**).

Electron microscopic examination of the renal cortices of the control rats demonstrated regular Bowman's membrane, lined by a single layer of parietal cells (**Figure 4**). The visceral epithelial cells (podocytes) appeared large with large nuclei and their cytoplasm contained rough endoplasmic reticulum (**Figure 4**). From podocytes extended primary major processes which gave rise to numerous secondary minor processes that ended by foot processes resting on the capillary basement membrane (**Figure 4**). The glomerular capillaries were lined by a thin layer of endothelial cells containing nuclei bulging into the capillary lumen (**Figure 4**). A branched dense mesangial substance containing mesangial cells provided support for the capillary loops (**Figure 4**). The Bowman's space between the parietal epithelium and podocytes appeared clear without any cellular debris (**Figure 4**).

Ultrastructural examination of the proximal convoluted tubules of control rats (**Figure 5**)

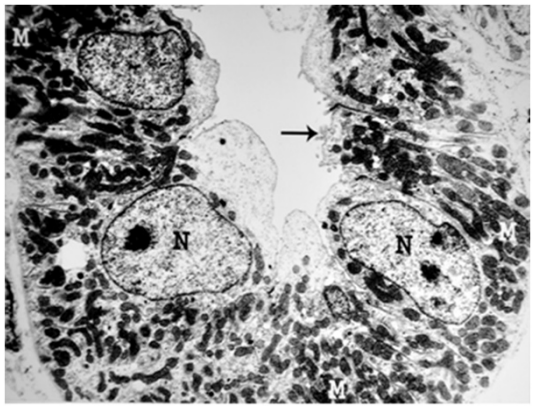


**Figure 6.** An electron micrograph of a renal cortex of a control albino rat, showing a distal convoluted tubule which is lined by cubical cells with few microvilli (arrow) and large nuclei (N) close to their luminal surface. Large numbers of mitochondria (M) are situated in the basal parts of the cells (Uranyl acetate and lead citrate: X 5000).

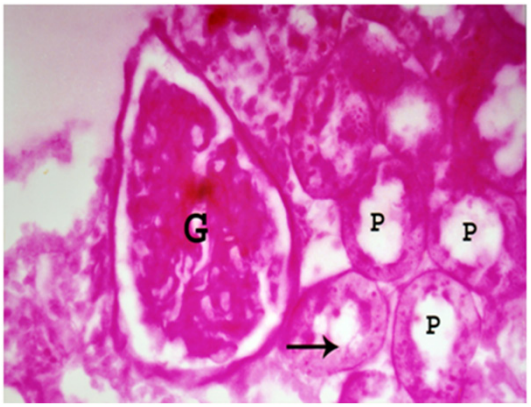


**Figure 7.** A photomicrograph a section of renal cortex of albino rat from group III showing deformity of glomerular tuft (G). The proximal convoluted tubules (P) reveal patchy loss of brush border (arrow) (PAS reaction; X 400).

showed that they were lined by cells with profuse luminal microvilli, constituting the brush border seen with light microscopy. Their nuclei were large, rounded with peripheral chromatin condensations. The cytoplasm immediately beneath the microvilli contained many pinocytic vesicles and lysosomes. The basal cell membrane exhibited deep basal infoldings into the cell. These infoldings were closely related to columns of elongated mitochondria situated longitudinally in the basal portions of the cells, oriented parallel to the cell axis (**Figure 5**).

By electron microscopy, the distal convoluted tubules of the renal cortices of the same rat

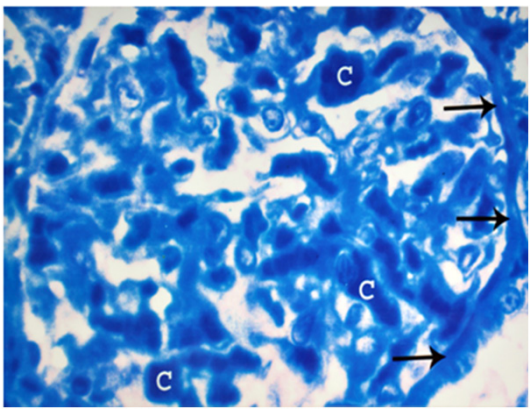


**Figure 8.** A photomicrograph of a semithin section of a renal cortex of albino rat from group III, showing dilatation and congestion of glomerular capillaries (C). Note obliteration of the Bowman's space and thickening with irregularity of Bowman's basement membrane (arrows) (Toluidine blue X 1000).

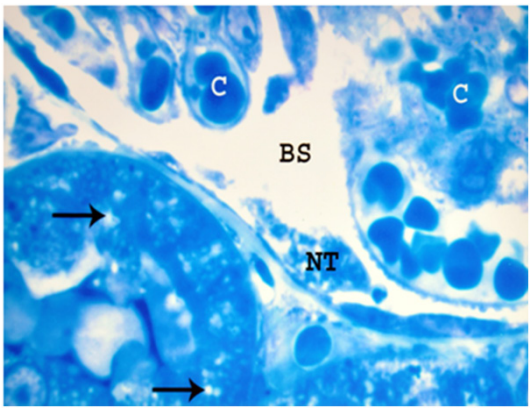


**Figure 9.** A photomicrograph of a semithin section of a renal cortex of albino rat from group III, showing dilated and congested glomerular capillaries (C). Bowman's space (BS) is dilated and containing necrotic tissues (NT). The proximal convoluted tubules reveal pleomorphic vacuoles (arrows) in the cytoplasm (Toluidine blue X 1000).

group (**Figure 6**) revealed that they were lined by cubical cells with few irregular small luminal microvilli. The nuclei were large, close to the luminal surface of the cells and consequently tended to bulge into the lumen. A large number of mitochondria were situated in the basal parts of the cells (**Figure 6**).

*Group II:* Light microscopic examination of the renal cortices of rats in group II revealed deformity of the glomerular tuft (**Figure 7**) and congestion of glomerular capillaries (**Figures 8**, **9**). Obliteration of Bowman's space with thickening

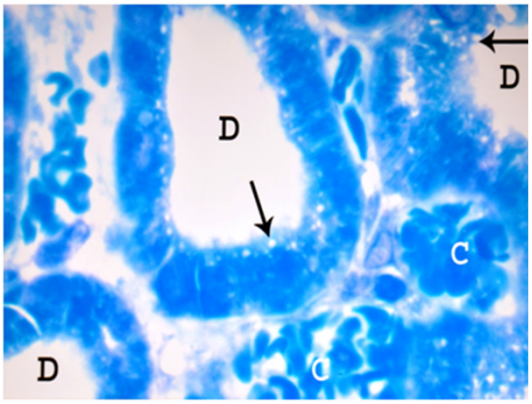


**Figure 10.** A photomicrograph of a semithin section of a renal cortex of albino rat from group II showing distal convoluted tubules (D) with marked peritubular congestion (C) and apical vacuolation (arrows) (Toluidine blue X 1000).

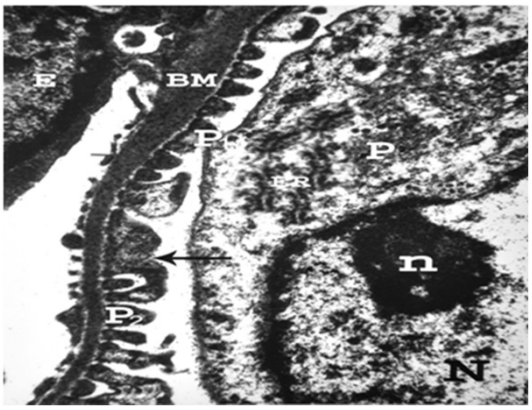


**Figure 11.** An electron micrograph of a renal cortex of albino rat from group III, showing part of a glomerulus with endothelial cell (E) resting on thick glomerular basement membrane (BM). Note podocytes (P) with its rough endoplasmic reticulum (ER), large nucleus (N) with its peripheral nucleolus (n) normal major process ($P_1$) and fusion (arrow) of some secondary foot processes ($P_2$) (Uranyl acetate and lead citrate X 12000).

and irregularity of Bowman's basement membrane were observed (**Figure 8**). In some specimens, necrotic tissues were noticed in dilated Bowman's space (**Figure 9**). The proximal convoluted tubules showed patchy loss of the brush border (**Figure 7**). Some cells of the proximal convoluted tubules showed pleomorphic vacuoles in the cytoplasm (**Figure 9**). On the other hand, peritubular congestion and apical vacuolation were observed in the distal convoluted tubules (**Figure 10**).

On electron microscopy, there was mild thickening of the glomerular basement membrane

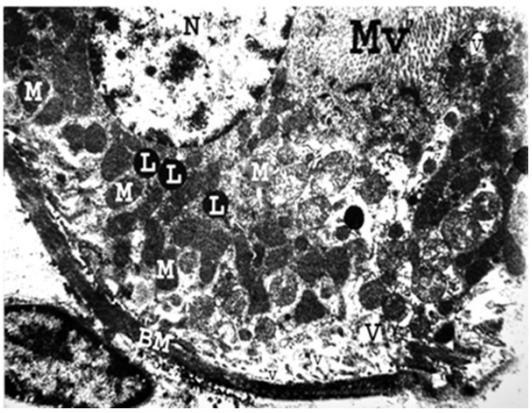


**Figure 12.** An electron micrograph of a renal cortex of albino rat from group III, showing part of a cell lining the proximal convoluted tubule that has a thick tubular basement membrane (BM) with absence of its normal basal infoldings and loss of parallel arrangement of mitochondria (M). Pleomorphic cytoplasmic vacuoles (V) are seen. Note the presence of normal nucleus (N), lysosomes (L) and microvilli (MV) (Uranyl acetate and lead citrate X 5000).

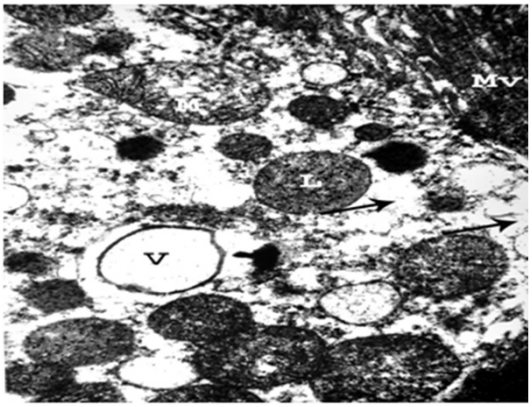


**Figure 13.** An electron micrograph of a renal cortex of albino rat from group III showing the apical part of a cell lining the proximal convoluted tubule with large vacuole (V) and irregular destruction (arrows) of the cytoplasm. Mitochondrial swelling (M) with destruction of its cristae and lysosomal swelling (L) are seen. Normal microvilli (MV) are noticed (Uranyl acetate and lead citrate; X 10,000).

(**Figure 11**). Mild changes were observed in the podocytes which had rough endoplasmic reticulum, normal nuclei with abnormal prominent peripheral nucleoli and normal major processes but abnormal fusion of some secondary foot processes could be detected (**Figure 11**). At the same time, there were mild thickening of the basement membrane of the proximal convoluted tubules and loss of its basal infoldings (**Figure 12**). Pleomorphic cytoplasmic vacuoles

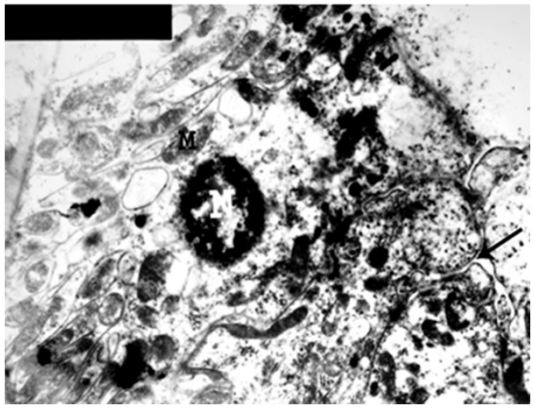


**Figure 14.** An electron micrograph of a renal cortex of albino rat from group III showing a cell lining the distal convoluted tubule with small atrophic nucleus (N), swelling of mitochondria (M) and obliteration of tubular lumen (arrow) (Uranyl acetate and lead citrate X 5000).

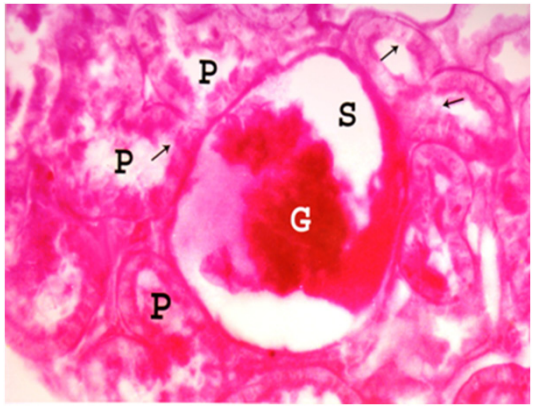


**Figure 15.** A photomicrograph of a section of a renal cortex of albino rat from group IV, showing distorsion, destruction and shrinkage of glomerular tuft (G) with wide irregular Bowman's space (S). There is extensive loss of the brush border (arrows) of proximal convoluted tubules (P) (PAS reaction; X 400).

and loss of normal parallel basal arrangement of mitochondria in the proximal tubules was noticed (**Figure 12**). Some proximal convoluted tubules revealed irregular destruction of the cytoplasm, mitochondrial swelling with destruction of its cristae, and lysosomal swelling (**Figure 13**). On the other side, small atrophic nuclei, swelling of mitochondria, and obliteration of tubular lumen were observed in the distal convoluted tubules (**Figure 14**).

*Group III:* Light microscopic examination of the rat renal cortices in this group showed distortion, destruction and shrinkage of glomerular

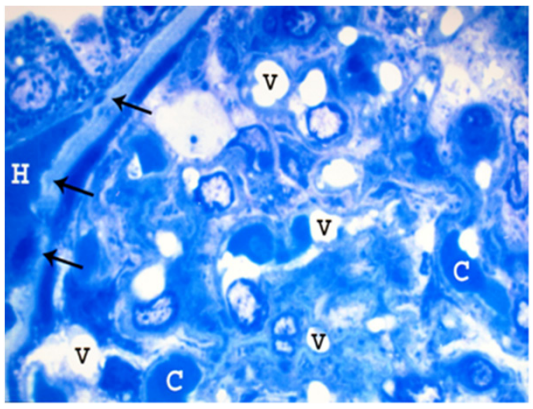


**Figure 16.** A photomicrograph of a semithin section of a renal cortex of albino rat from group IV, showing part of a glomerulus with obliteration of Bowman's space as well as congestion and dilatation of glomerular capillaries (C). Multiple vacuoles (V) in the glomerulus, and periglomerular haemorrhage (H) are also noticed. Note irregular thickening in the Bowman's membrane (arrows) (Toluidine blue; X 1000).

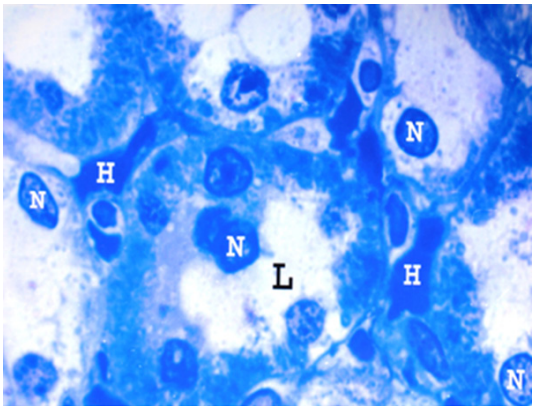


**Figure 17.** A photomicrograph of a semithin section of a renal cortex of albino rat from group IV, showing proximal convoluted tubules with apical destruction of the tubular cells and migration of the nuclei (N) towards the wide lumen (L). Note the peritubular haemorrhage (H) (Toluidine blue X 1000).

tuft with wide irregular Bowman's space (**Figure 15**). Some glomeruli revealed congestion and dilatation of glomerular capillaries (**Figure 16**). Multiple vacuoles in the glomeruli and periglomerular haemorrhage were observed (**Figure 16**). Obliteration of Bowman's space and irregular thickening of Bowman's membrane were also noticed (**Figure 16**). The proximal convoluted tubules showed extensive loss of brush border (**Figure 15**). Many cells lining the proximal convoluted tubules exhibited apical destruction and apical migration of their nuclei

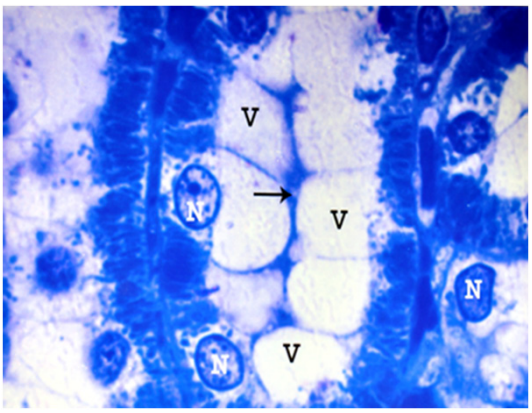


**Figure 18.** A photomicrograph of a semithin section of a renal cortex of albino rat from group IV, showing distal convoluted tubule with apical vacuolation (V), obliteration of the lumen (arrow) and basal location of the nuclei (N) (Toluidine blue; X 1000).

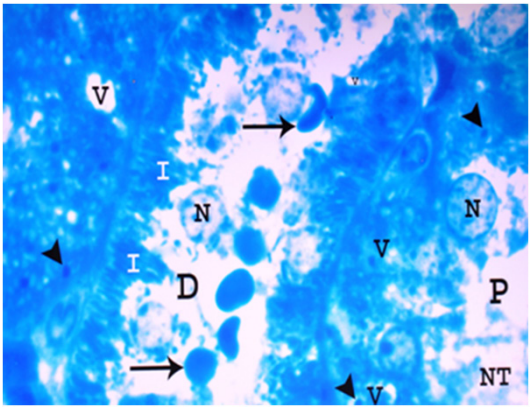


**Figure 19.** A photomicrograph of a semithin section of a renal cortex of albino rat from group IV, showing parts of proximal (P) and distal (D) convoluted tubules with destruction of tubular cells, apical direction of the nuclei (N) , necrotic tissues (NT) and red blood cells (arrows) in the lumen. Irregular basal invaginations (I) into the cytoplasm, pleomorphic vacuoles (V) and dense bodies (arrow heads) are noticed (Toluidine blue X 1000).

(**Figure 17**). Peritubular haemorrhage was also noticed (**Figure 17**), while apical vacuolation, obliteration of the lumen and basal location of the nuclei were observed in the distal convoluted tubules (**Figure 18**). Furthermore, severe changes occurred in some proximal and distal convoluted tubules in the form of destruction of their cells, apical direction of the nuclei, irregular basal invaginations into the cytoplasm, pleomorphic vacuoles and dense bodies in the cytoplasm with necrotic tissues and red blood cells in their lumina (**Figure 19**).

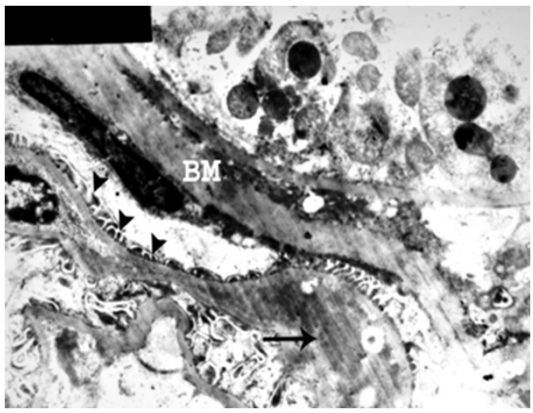


**Figure 20.** An electron micrograph of a renal cortex of albino rat from group IV showing part of a glomerulus with marked irregular thickening of the capillary basement membrane (arrow), marked thickening of Bowman's membrane (BM) and few small atrophic secondary foot processes (arrow heads) (Uranyl acetate and lead citrate; X 4000).

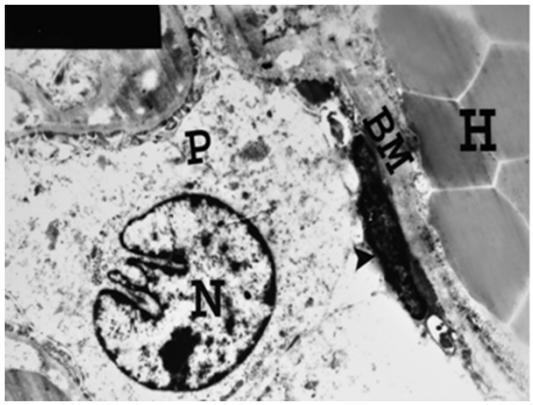


**Figure 21.** An electron micrograph of a renal cortex of albino rat from group IV, showing part of a glomerulus with marked thickening of Bowman's membrane (BM), atrophy of parietal cell (arrow head) and obliteration of Bowman's space. Note the podocyte (P) with its irregular nucleus (N). Periglomerular haemorrhage (H) is also noticed (Uranyl acetate and lead citrate; X 4000).

Electron microscopic examination of the rats renal cortices belonging to group III revealed marked irregular thickening of capillary basement membrane with few small atrophic secondary foot processes (**Figure 20**). Marked thickening of Bowman's membrane, atrophy of parietal epithelial cells of Bowman's capsule, obliteration of Bowman's space and irregular deformed nuclei of podocytes were observed (**Figure 21**). Periglomcrular haemorrhage was also noticed (**Figure 21**). The proximal convo-

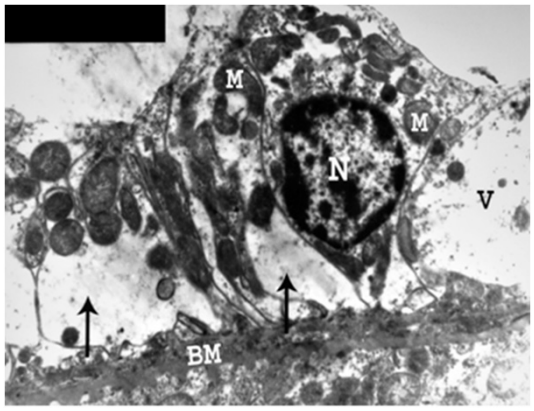


**Figure 22.** An electron micrograph of a renal cortex of albino rat from group IV, showing a cell lining a proximal convoluted tubule with marked thickening of basement membrane (BM) and absence of its basal infolding. There are destruction of basal cytoplasm (arrows), marked vacuolation (V) and migration of mitochondria (M) towards the lumen with loss of their parallel arrangement. Note absence of luminal microvilli and presence of a normal nucleus (N) when compared to the control (Uranyl acetate and lead citrate; X 5,000).

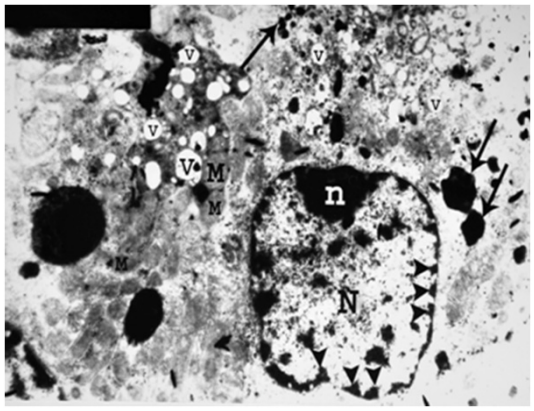


**Figure 23.** An electron micrograph of a renal cortex of albino *rat from* group IV, showing a *cell lining* a proximal convoluted tubule with few swollen mitochondria (M), pleomorphic vacuolation (V) and heterogenous irregular dense bodies mostly lysosomes (arrows). Note the nucleus (N) and marginal nucleolus (n) with fragmentation and migration of chromatin with areas of karyolysis (arrow heads) (Uranyl acetate and lead *citrate*; X 5000).

luted tubules showed marked thickening of the basement membrane with absence of its normal basal infoldings (**Figure 22**). Disarrangement and migration of the mitochondria towards the lumen, destruction of basal cytoplasm, marked vacuolation in the cytoplasm and absence of luminal microvilli were detected in some proximal convoluted tubules (**Figure 22**). Some nuclei revealed fragmentation and migration of chromatin with areas of karyolysis. Pleomorphic vacuoles and heterogenous irregular dense bodies mostly lysosomes appeared in some of these tubules (**Figure 23**). Many cells lining the distal convoluted tubules exhibited destruction of their apical parts, apical direction of the nuclei with prominent peripheral nucleoli, swelling of mitochondria, thickening of basement membrane, presence of pleomorphic dense bodies mostly lysosomes and tissue debris in the lumen (**Figure 24**).

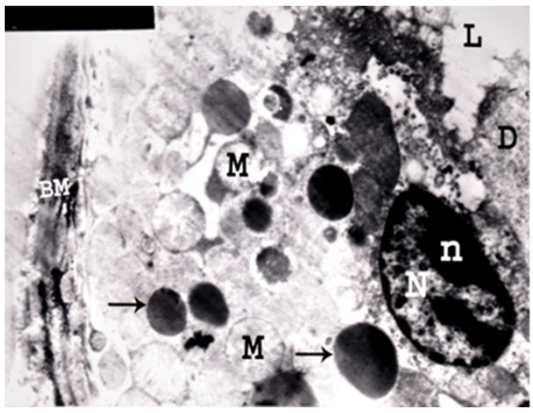


**Figure 24.** An electron micrograph of a renal cortex of albino rat from group IV showing a cell lining a distal convoluted tubule with destruction of its apical part, apical direction of its nucleus (N), prominent peripheral nucleolus (n), swelling of mitochondria (M) and thickening of its basement membrane (BM). Pleomorphic dense bodies mostly lysosomes (arrows) are seen in the cytoplasm. Tissue debris (D) is noticed in the lumen (L) (Uranyl acetate and lead citrate; X 5,000).

*Laboratory results*

In the experimental group II, there was a significant increase in the serum levels of urea, creatinine and electrolytes as compared with the control group.

On the other hand, there was a highly significant increase in all the examined parameters in the experimental group III as compared with the control group (**Table 1**).

## Discussion

Antimony is an environmental toxin present in air, water, food and soil as well as it is widely used in the manufacture of rubber, glass,

**Table 1.** Statistical analysis of blood urea, serum creatinine, serum potassium and serum sodium in the control groups (Ia & Ib) and the experimental groups (II and III)

| | Group Ia | Group Ib | | Group II | | Group III | |
|---|---|---|---|---|---|---|---|
| | Mean+SD | Mean+SD | P | Mean+SD | P | Mean+SD | P |
| Blood urea mg/100 ml | 38.41+1.01 | 38.4+0.7 | >0.05 | 47.38+0.87 | <0.05 | 79.5+0.37 | <0.01 |
| Serum creatinine mg/100ml | 0.74+0.05 | 0.76+0.06 | >0.05 | 1.53+0.03 | <0.05 | 2.24+0.004 | <0.01 |
| Serum potassium m.mol/L | 4.17+0.6 | 4.19+0.5 | >0.05 | 5.7+0.17 | <0.05 | 9.34+0.64 | <0.01 |
| Serum sodium m.mol/L | 140.3+4.99 | 140.3+5.11 | >0.05 | 149.62+0.6 | <0.05 | 172.4+0.71 | <0.01 |

Note: SD=Standard deviation; >0.05: insignificant; <0.05: significant; <0.01: highly significant.

paints, coatings and colored printing inks [25]. The nephrotoxicity of antimony has been recently suggested by many authors [2, 14].

Exposure to high antimony level in humans is rare, resulting in serious renal damage including destruction of its tubules, haemorrhage and renal failure [26]. On the other hand, subclinical antimony poisoning from chronic low level antimony exposure remains a major health problem especially in industrial workers [27]. Improvements in working conditions have remarkably decreased the incidence of antimony toxicity in the workplace [14].

The antimony was chosen as the target for this study as it is recent and one of the most dangerous heavy metals that can insult the environment [11]. The importance of antimony nephrotoxicity is resulting from its possible chronic ingestion over long periods by millions of general population all over the world and its possible potential hazards to the human health [28]. Therefore, the current study is designed to evaluate the effects of antimony administration on the structure and function of the renal cortex of growing albino rats.

Growing albino rats were used as a mammalian model for studying the possible effects of antimony, as they are available and easy in handling [29]. It was noticed that there were species and strain difference in antimony toxicity; albino rats were more sensitive to its toxicity than mice, guinea pigs and dogs [30].

The renal cortex of albino rats was used in this work as it is responsible for 83.8% of renal function, the main site of excretion of antimony and its metabolites and the first site to be damaged by their toxicity [31]. By autoradiography, it was found that the distribution of antimony in the kidney was not uniform and its deposition was more in the renal cortex than the medulla *and the* highest concentration was observed *in the proximal* and distal convoluted tubules [20]. Therefore, the glomeruli might be affected secondary to tubular damage [32].

In the present work, antimony trisulfide in low dose (6 mg/Kg body weight) was used. Since many authors suggested that the effect of antimony on the kidney could be attributed to antimony-induced malnutrition and not due to the direct influence of environmental antimony burden on the renal tissues, therefore the dose used in this study was adjusted not to alter the body weight or induce growth retardation and malnutrition [33]. In addition, this low dose of antimony was adjusted to avoid animal death and this dose is also similar to the antinomy environmental level in water in many places all over the world including many areas in the Arabic countries [14]. It was recorded that in acute antimony intoxication, the lethal dose of antinomy trisulphide causing death to 50% of rats ($LD_{50}$) was 600 mg/kg body weight [19].

The route of administration in the present study was via drinking water because it is the commonest route for antimony intoxication [34]. Adjustment of blood antimony level was not considered because the aim of this work was to expose the rats to low doses of antimony which are unnecessary to be constant to simulate the environmental exposure pattern.

In the experimental group II, the duration of exposure to antimony was eight weeks, was chosen to study the effects of antimony as a heavy metal added to drinking water [18]. In addition, 12 weeks was used in group III to study the possible effects of prolonged intake of antimony contaminated drinking water [13].

Changes in Malpighian renal corpuscles were noticed in all tested renal cortices in this experiment following antimony administration.

Glomerular changes appeared in the form of distortion, destruction and shrinkage of glomerular tuft with irregular glomerular space. Some glomeruli revealed congestion, thickening of their basement membrane, multiple vacuoles, and periglomerular haemorrhage. Obliteration of Bowman's space, irregular thickening of Bowman's membrane and abnormal fusion with atrophy of some secondary foot processes of the podocytes, could be also detected. These observations are close to those recorded by other researchers [26, 35]. The latter authors also noticed abnormal proliferation of parietal cells of Bowman's capsule which might predispose to malignancy in case of chronic use of antimony. This finding was not observed in this study, a point needs prolonged administration of antimony in further investigations. On the contrary denied any abnormality in the Malpighian renal corpuscles after the intake of antimony for 8 weeks [1].

The current investigation revealed variable changes in the proximal convoluted tubules following antimony administration. Marked thickening of tubular basement membrane with absence of its normal basal infolding, disarrangement and migration of mitochondria towards the lumen and destruction with vacuolation of cytoplasm were also detected. These findings are in accordance with those reported by other reporters [36, 37]. The primary effect of antimony on the kidney was in the proximal convoluted tubules due to their ability to concentrate this substance and its toxic metabolites leading to electric changes and disturbance in the tubular reabsorption active transport system [6].

This research showed that antimony administration resulted in many changes in the distal convoluted tubules in the form of cytoplasmic vacuolation, atrophy of nuclei, mitochondrial swelling, obliteration of tubular lumen and peritubular haemorrhage. Many distal convoluted tubules revealed apical destruction of their cells, apical direction of nuclei, thickening of basement membrane and presence of tissue debris in dilated lumen. These observations are in agreement with the results of authors who also mentioned that antimony nephrotoxicity affected distal convoluted tubules secondary to morphological changes in the proximal convoluted tubules [1].

The present study noticed marked damage of the tubular brush border as evidenced by PAS technique and electron microscopic examination. The severity of antimony induced tubular brush border damage was previously tested by [38], using trehalase enzyme which is localized in the brush border. The same authors concluded that urinary trehalase activity was elevated in tubular degeneration induced by antimony and such elevation in enzymatic activity was proved to be very sensitive indicator of direct morphological damage of tubular brush border.

The current study revealed congestion of blood vessels and haemorrhage in the renal cortex. The actual causes of these changes induced by antimony intake remained obscure [16]. Other's results are in consistency with ours who mentioned that antimony has a direct toxic effect on the wall of small blood vessels leading to vasodilatation and extravasation of blood from their necrotic walls [27].

The present research showed multiple cytoplasmic vacuoles representing cellular oedema which was recognized in most tubular cells. This observation is in accordance with others who attributed this finding to disturbance in cellular calcium due to the extreme sensitivity of the calcium pumping ATP-ase which was found in both plasma membrane and endoplasmic reticular membrane [12]. Cellular edema was due to disruption of intracellular pH which regulated ion transport systems and played an important role in many cell functions such as energy metabolism, DNA and RNA synthesis, and induction of cellular proliferation [6].

The present work revealed that effects of antimony on the renal cortex of albino rats appeared at the tubular as well as the glomerular levels simultaneously. These findings are in contrast to the observations of others who recorded that the nephrotoxic effect of antimony was observed first at the level of proximal convoluted tubules, then at the distal convoluted tubules, and finally at the glomerular level [39].

The current experiment demonstrated that the effects of antimony on the cells of the glomeruli and the tubules were patchy and uneven in distribution. This can be explained in the light of the results of researchers who observed that there was variable susceptibility of cortical

cells to the nephrotoxic effect of antimony which depended on the chemical receptors within these cells [17].

The prolonged use of antimony and some other heavy metals might be carcinogenic and cause malignancy in the kidney, urinary bladder, liver, stomach, colon or rectum [1, 24]. Moreover, it was also recorded that continuous oral administration of antimony for six months resulted in diffuse hyperplasia and focal neoplasia in the stomach, colon and kidney [20]. Antimony lowered acidity of urine and increased urinary tract bacteria which reduced urinary nitrate to nitrite with the formation of N-nitroso compounds which would be carcinogenic to the renal epithelium of many animal species and human being [27]. On the other hand, the occurrence of any renal cell neoplasia as a result of continuous administration of antimony has been denied [7]. The current study could not detect any manifestations of hyperplasia, dysplasia or malignant transformation of the renal cells of albino rats. A longer period of continuous administration of antimony may be required to confirm such malignant changes; a point that needs further investigation.

The laboratory investigations in the current study demonstrated that administration of antimony was toxic on the kidney being evidenced by significant increase in all investigated parameters. The degree of this toxicity was directly proportional to the duration of exposure of antimony. These findings are in agreement with the histological observations in the present study. These results are in accordance with the reports other reporters who also added that this toxicity was dose dependent and described similar toxic effects in the liver cells of rats following antimony administration [36]. The affection of the ultrastructure of the renal tubules of albino rats following antimony administration did not stop after its withdrawal [5]. In antimony treated rats, the degenerative effects on the renal cortical cells increased after drug withdrawal to be maximal 30 days after the last dose [15].

The possible mechanism of antimony toxicity on the kidney is due to its deposition with its toxic metabolites within the renal tubules [40]. Confirmation of this view by using immunofluorescence technique also has been done [12]. On the other hand, others believed that the mechanism of antimony nephrotoxicity was still unknown whether due to changes in the tubular active transport system or capability for effective concentration [41].

Considering the results of the current study and correlating them to those of other investigators, it can be concluded that antimony has proven to be toxic on the structure and function of the renal cortex of growing albino rat. On the other hand, hyperplasia, dysplasia and malignant changes could not be detected following continuous oral administration of antimony for 8 and 12 weeks. These changes could not be demonstrated as longer duration or different dose for administration, than that used in this study, was needed.

Based on the results of the present study, it should be recommended to avoid the use of any drinking water contaminated with antimony compounds and forbidden its use in infants and children foods. Also, avoid daily consumption of any contaminated water to prevent the accumulation of antimony compounds in body tissues and the internal organs. Lists for permitted substances in drinking water have to be prepared in view of the recent findings concerning the safety aspects of heavy metals. Using of antimony compounds in different industries should be under the governmental control. Synthetic substances used in human diets must be defined clearly and further studies on its structure, metabolic action and toxicological properties should be undertaken. Stress should be made on orienting parents to the importance of the household meals and its role in improvement of food habits for their children. Nutritional education programs should be carried out to limit the consumption of processed products with unhealthy contaminated water especially among children. Advertisement on streets, snack and restaurants foods have to be done under strict supervision. Educational messages have to be published in television, newspapers, magazines and internet concerning the health hazards associated with the liberal use of water contaminated with antimony and other heavy metals.

**Acknowledgements**

This work was supported by Taif University, Taif, kingdom Saudi Arabia (grant number 1931\433\1).

**Address correspondence to:** Dr. Ayman K Ismail, Department of Clinical Pharmacology, Forensic Medicine and Toxicology section, College of Medicine, Taif University, Taif, Saudi Arabia. Phone: 00966 02 7272966, ext. 1035; Cellular: 00966 0530049672; E-mail: aykam4@yahoo.com; aymanka@tu.edu.sa

## References

[1] Abadin HG, Murray HE, Wheeler JS. The use of hematological effects in the development of minimal risk levels. Regul Toxicol Pharmacol 1998; 28: 61-66.

[2] Kale RM. Genotoxic effects of antimony on rat and mice. J Appl Toxicol 2011; 25: 17-20.

[3] Marc SB, Gonzalez HP, Obregon ER. Mechanisms of selective action of heavy metal toxicity. Ann Rev Pharmacol Toxicol 2012; 63: 321-327.

[4] Aboel-Zahab H, el-Khyat Z, Sidhom G, Awadallah R, Abdel-al W, Mahdy K. Physiological effects of some synthetic food coloring additives and heavy metals on rat. Chim Farm 1997; 136: 615-627.

[5] Adda J, Roger S, Dumont J. Modulating effect of antimony and vanillin in a rat medium term multi-organ carcinogenesis model. Cancer Letters 2003; 104: U3-121.

[6] Lake BG, Price RJ, Cun-nigham ME, et al. Comparison of the effect of antimony on hepatic peroxisome proliferation and cell replication in the rat and mouse. Fundam Appl Toxicol 2004; 52: 60-66.

[7] Sasaki YF, Kawaguchi S, Kamaya A, Ohshita M, Kabasawa K, Iwama K, Taniguchi K, Tsuda S. The Comet assay with 8 mouse organs: results with 39 currently used metals. Mutat Res 2002; 519: 103-119.

[8] Wang TB, Yang RC, Chen JH, et al. Effect of antimony on the blood-brain barrier function and oxidative damage on selected organs of developing rats. Reprod Nutr Dev 2010; 45: 572-581.

[9] Rogers WB, Davis DJ. Antimony and child development. Nature 2011; 358: 183-205.

[10] Doyle WH. Nutritional status of school children in an inner city area. Arch Dis Childhood 1997; 70: 376-381.

[11] Koutso PL, Maravelias CF, Koutselinis AJ. Immunological aspects of the common heavy metals, amaranth and tartrazine. Hum Toxicol 1998; 40: 11-24.

[12] Reitman S, Frankel S. Hypothalamic lesions after antimony injection in newly born primates. Science 2001; 272: 1702-1708.

[13] Adams RL, Knowler JT, Leader DP. Effect of some synthetic antimony compounds on blood hemoglobin and renal function of rats. Science 2004; 262: 673-692.

[14] Flower CA. Antimony poisoning management. Clin Toxicol Rev 2009; 32: 16-21.

[15] Shahidi F. Chronic heavy metals toxicity studies in rats, guinea pig and monkeys. Indian J Exp Biol 2004; 83: 77-83.

[16] Christian MS, Parker RM, Hoberman AM, Diener RM, Api AM. Developmental toxicity studies of four heavy metals in rats. Toxicol Lett 1999; 111: 169-174.

[17] Adams NJ, Ranter AD. Comparative studies on carbohydrate and lipid metabolism in rats administrated antimony. N Engl J Med 2002; 384: 1782-1789.

[18] Reyes FG, Valim MF, Vercesi AE. Effect of organic synthetic antimony on mitochondrial respiration. Food Addit Contam 2003; 18: 5-11.

[19] Wolfe BR, Molinoff PB. Heavy metal toxicity in the 21st. Century Toxicology 2012; 85: 125-129.

[20] Tsuda SK, Sasaki YZ. DNA damage induced by antimony orally administrated to pregnant and male mice. Toxicol Sci 2001; 61: 92-99.

[21] Smith JM. Adverse reactions to food and drug additives. European J Clin Nutr 1999; 55: 17-21.

[22] Bancroft JD, Stewens A, Devvson MP. Theory and practice of Histological Technique. 6th edition. Edinburgh, London and New York: Churchill Livingstone 2009; pp: 173-184.

[23] Drury RA, Wallington EA. Carleton's Histological Technique. 9th edition. Oxford, New York, Toronto: Oxford University Press 2009; pp: 139-142.

[24] Meek GA. Practical Electron Microscopy for Biologists. 4th edition. New York, Brisbane, Toronto and Sans: 1990; pp: 413-429.

[25] Toxicological evaluation of some heavy metals. FAO/WHO. Food Agric. Org. Of the United Nations & World Health. Org. Rome. 2000; 22-37.

[26] Ferguson JE, Beck MH. Contact sensitivity to antimony in a lip slave. Contact Dermatitis 2000; 33: 352-361.

[27] Domingo JL. Health risks of synthetic and genetically modified foods. Science 2001; 288: 1748-1759.

[28] Cray J, Buttriss J. Maternal and Fetal nutrition. National Dairy Council Nutrition Service 1999; 11: 157-184.

[29] Taylor SL, Dormed ES. Flavorings and colorings. Food Allergy Research and Resource Program. University of Nebraska, Lincolin USA. Allergy 1998; 53: 80-92.

[30] Wuthrich B. Adverse reaction to food additives. Ann Allergy 1999; 71: 379-384.

[31] Onoa M, Oliven A. Changes in blood electrolytes and metabolites among adult rats treated

with a nephrotoxic dose of antimony. Life Sci 2000; 28: 2855-2864.
[32] Taylor DL, Larick DK. Chemists define flavor in many ways. Food Technol 2001; 22: 1360-1365.
[33] Ford RA, Domeyer B, Maier K. Criteria for development of a data base for safety evaluation of heavy metals. Regul Toxicol Pharmacol 2000; 31: 166-181.
[34] Barnes SG. Planning For a Healthy Baby. 4th edition. London: Ebury Press 1998; pp: 112-153.
[35] Schiffman SS, Warwick ZS. Effect of flavor enhancement of foods for the elderly on nutritional status: food intake, biochemical indices and anthropometric measures. Physiol Behav 1998; 531: 395-402.
[36] Trinder P. The metabolism of antimony compounds: A review of the literature. Food Cosmet Toxicol 1999; 18: 659-671.
[37] Shahidi F, Rubin LJ, Dsouza LA. Antimony: A review of the composition, techniques of analysis and sensory evaluation. Rev Food Sci Nutr 2003; 24: 18-24.
[38] Kroes R, Koziano G. Threshold of toxicological concern (TTC) in heavy metals safety assessment. Toxicol Lett 2002; 127: 43-46.
[39] Weibel H, Harsen JS. Chemical reaction of antimony with protein. J Clinic Gastroentrol 2002; 35: 254-261.
[40] Munro IC, Shubik PT, Hall RW. Principles for the safety evaluation of heavy metals. Food and Chem Toxicol 1998; 36: 529-540.
[41] Munro TG, Kennepohl EJ. Effect of daily intake of heavy metals. Food and Chem Toxicol 2004; 39: 331-354.